

Formation energy of Cr/Al vacancies in spinel MgCr_2O_4 and MgAl_2O_4 by first-principles calculations

Hiroki Moriwake,¹ Isao Tanaka,¹ Fumiyasu Oba,² Yukinori Koyama,¹ and Hirohiko Adachi¹

¹*Department of Materials Science and Engineering, Kyoto University, Sakyo, Kyoto, 606-8501 Japan*

²*Engineering Research Institute, The University of Tokyo, Bunkyo, Tokyo 113-8656, Japan*

(Received 27 February 2001; revised manuscript received 24 January 2002; published 29 March 2002)

First-principles pseudopotential calculations using plane-wave basis functions have been made to quantitatively evaluate the formation energy of Cr/Al vacancies in MgCr_2O_4 and MgAl_2O_4 . Relaxation of atoms within the second nearest neighbor shell of the vacancy was taken into account in a 56-atom supercell. The formation energy was calculated as a function of the atomic chemical potential of Cr/Al. It shows negative values in the case of the oxidation limit of MgCr_2O_4 , which is in good agreement with experimental results showing abundance of Cr vacancies when annealed in air. On the other hand, the formation energy of the Al vacancy in MgAl_2O_4 under the same condition is as large as 4.76 eV. This also well corresponds to the experimental fact that MgAl_2O_4 does not form the Al vacancy alone in air.

DOI: 10.1103/PhysRevB.65.153103

PACS number(s): 71.20.Ps, 71.55.Ht, 61.72.Ji

I. INTRODUCTION

Magnesium chromate $\text{MgCr}_{2-x}\text{O}_4$ with a spinel structure is known to show wide nonstoichiometry in the range of $0 < x < 0.49$ at 2300 °C by the formation of Cr vacancies.¹ The sintered $\text{MgCr}_{2-x}\text{O}_4$ material has been used commercially to monitor the temperature of exhaust gas in automobiles, since it exhibits *p*-type electric conductivity which is stable at temperatures around 1000 °C in air.²⁻⁴ We have previously reported results of first-principles molecular orbital calculations using model clusters.⁵ A comparison between MgCr_2O_4 and its isostructural compound MgAl_2O_4 was made in order to extract the peculiarity of MgCr_2O_4 , although noncompensated Al vacancy is unlikely to occur in MgAl_2O_4 . Population analyses by the Mulliken's scheme⁶ were systematically made in order to examine the spatial distribution of holes associated with metal vacancies and the changes in chemical bonding around the vacancy. Discussion on the electronic mechanism behind the abundance of the Cr vacancies in MgCr_2O_4 was then made.

The holes associated with the Al vacancy were found to localize on the neighboring oxygen ions in MgAl_2O_4 . On the other hand, spatial distribution of holes was found to be much wider in the case of the Cr vacancy in MgCr_2O_4 . It was localized not only on the neighboring oxygen ions, but also on Cr ions in the vicinity of the Cr vacancy. Covalent bonding between Cr and O was remarkably reinforced by the formation of the Cr vacancy in MgCr_2O_4 . At the same time the decrement of the ionic bonding was much smaller also in MgCr_2O_4 . These two factors were pointed out to play key roles for the abundance of Cr vacancies in MgCr_2O_4 as compared with MgAl_2O_4 . Although our previous work provided an insight for the electronic mechanism to form the vacancy, no quantitative information was given. Local atomic relaxation around the vacancies was not taken into consideration, either. The present study is made to verify the idea in a quantitative manner using a first-principles supercell approach. The plane-wave pseudopotential method is employed since it is an accurate and efficient tool to quantify the

atomic relaxation around the vacancies in a complex system. This gives the complementary information to the previous study. The cluster calculations use minimal number of atomic basis functions, which provides a straightforward interpretation of the change in chemical bonding. On the other hand, the supercell approach with sufficient number of plane-wave basis functions has an advantage in the efficient evaluation of structure optimization and total energies.

II. COMPUTATIONAL PROCEDURES

MgCr_2O_4 is known to exhibit a normal spinel structure with a lattice parameter $a = 8.3378$ Å and an oxygen parameter $u = 0.386$.⁷ MgAl_2O_4 also shows spinel structure with $a = 8.0887$ Å and $u = 0.388$.⁸ Although MgAl_2O_4 often exhibits a mixed spinel structure with respect to tetrahedral and octahedral cation sites, we assumed a normal spinel structure for simplicity. Magnetic properties of MgCr_2O_4 have been investigated by several groups.⁹⁻¹³ It shows antiferromagnetism with a Néel temperature of 16 K. Despite these efforts, its detailed magnetic structure at the ground state is not well established. We have made full-potential linearized augmented plane wave (FLAPW) calculations¹⁴ of MgCr_2O_4 with both ferromagnetic and antiferromagnetic ordering of Cr atoms. The results differ in total energy by only 0.05 eV per MgCr_2O_4 . We have therefore assumed the ferromagnetic ordering in this study for simplicity and computational economy.

All calculations were performed within the generalized gradient approximation (GGA) (Ref. 15) of the density functional theory, using a plane-wave pseudopotential method.¹⁶ Multielectron interactions among localized *d* orbitals were ignored in the present study. Calculations for vacancies were made using the supercell composed of 56 atoms that is four times greater than the primitive cell. Ultrasoft pseudopotentials¹⁷ were employed with a plane-wave cutoff energy of 400 eV. The convergence of the vacancy formation energies with respect to the cutoff energy up to 800 eV was better than 0.01 eV for MgAl_2O_4 and 0.05 eV for MgCr_2O_4 . Numerical integration was carried out using two **k** points in

TABLE I. Theoretical interatomic distances around the Cr/Al vacancy before and after the relaxation for MgCr_2O_4 and MgAl_2O_4 .

	MgCr_2O_4			MgAl_2O_4		
	Before	After	Difference (%)	Before	After	Difference (%)
Vacancy-O	2.051 Å	2.272 Å	+10.8	1.903 Å	2.101 Å	+10.4
Vacancy-Al				2.85	2.825	-0.9
Vacancy-Cr	3.025	2.954	-2.3			
Vacancy-Mg	3.545	3.555	+0.3	3.342	3.347	+0.2
O-Al				1.903	1.931	+1.5
O-Cr	2.051	1.942	-5.3			
O-Mg	2.008	1.978	-1.5	1.952	1.829	-6.3

the irreducible part of the Brillouin zone, which is one fourth in volume. The convergence with respect to the number of \mathbf{k} points were better than that of the cutoff energy.

The self-consistent total energies were obtained by the density mixing scheme¹⁸ in conjunction to the conjugate gradient technique.¹⁹ Atomic positions were optimized using the quasi-Newton method with the Broyden-Fletcher-Goldfarb-Shanno Hessian update scheme.²⁰ Atomic arrangements around the vacancies were optimized allowing relaxation of the first and second nearest neighbors. The relaxation procedures were truncated when all the residual forces for the relaxed atoms were less than 0.1 eV/Å. We also carried out calculations of a number of reference materials, i.e., Mg(hcp), Al(fcc), Cr(bcc), crystalline O($C2/m$), $\text{Al}_2\text{O}_3(R\bar{3}c)$, $\text{Cr}_2\text{O}_3(R\bar{3}c)$, and $\text{MgO}(Fm\bar{3}m)$. The total energy of the reference materials were obtained after their structures were optimized by the same computational method for consistency. Theoretical lattice constants of these reference systems well reproduced their experimental values within an error of $\pm 3\%$.

III. RESULTS AND DISCUSSION

A. Perfect crystals of MgCr_2O_4 and MgAl_2O_4

We first performed calculations for the perfect crystals of MgCr_2O_4 and MgAl_2O_4 . There are only two parameters in the cubic spinel structure, i.e., the lattice parameter a and the oxygen parameter u . The parameters were optimized through the minimization of the total energies. Theoretical values of a were 8.550 Å for MgCr_2O_4 and 8.062 Å for MgAl_2O_4 . They agree with the experimental values of a , i.e., 8.3378 Å for MgCr_2O_4 and 8.0887 Å for MgAl_2O_4 , with errors of +2.5 and -0.3%, respectively. Theoretical u parameters were 0.385 and 0.390 for MgCr_2O_4 and MgAl_2O_4 , respectively. They also show satisfactory agreements with experimental values, i.e., 0.386 and 0.388, respectively.

The following quantity should correspond to the experimental enthalpy of formation if we neglect the entropy contribution:

$$\Delta H(\text{MgAl}_2\text{O}_4) = E_t(\text{MgAl}_2\text{O}_4) - [E_t(\text{Mg}) + 2xE_t(\text{Al}) + 4xE_t(\text{O})], \quad (1)$$

where E_t is the total energy of the compound per unit formula. Although experimental data are generally defined with $\text{O}_2(\text{gas})$ as a standard not with the solid O in the $C2/m$ structure,²¹ we found the difference in E_t between two is smaller than 0.04 eV/atom when the calculation of the O_2 molecule was made using a supercell $10 \times 10 \times 10$ Å³. Spin polarization was taken into account for O_2 . The theoretical value of 22.2 eV/unit formula is close to the experimental enthalpy of formation at 298 K, 21.8 eV.²² The theoretical value for MgCr_2O_4 is obtained to be 15.1 eV/unit formula. Experimental value is not available for MgCr_2O_4 .

B. Geometry and electronic structure around a Cr/Al vacancy

Calculations of the defective crystals were performed using a supercell containing 56 atoms. In order to model the system with infinitely dilute vacancy concentration, lattice constant a was fixed at the optimized value of the perfect crystal. Atomic arrangements around the vacancy were optimized allowing relaxation of the first and second nearest neighbors of the vacancy. Since we use a neutral supercell, the result corresponds to quantities for a neutral metal vacancy.

Interatomic distances before and after the atomic relaxation are listed in Table I. The vacancy position was defined as the position of the metal atom before its removal. In both compounds the distance between vacancy and the first nearest-neighbor oxygen largely increases. The distance between vacancy and the second nearest-neighbor Cr and Al decreases. The distance between vacancy and Mg shows little change. Remarkable difference between MgCr_2O_4 and MgAl_2O_4 can be found in the bond lengths of O-Cr/Al and O-Mg around the vacancy. In MgCr_2O_4 , the bond length of O-Cr decreases by 5.3%. On the other hand, the bond length of O-Al increases by 1.5% in MgAl_2O_4 . It is also interesting that the change in the bond length of O-Mg due to the relaxation is much greater in MgAl_2O_4 .

The remarkable difference in the bond lengths of O-Cr/Al may be explained from a simplified chemistry viewpoint. If we fix the oxidation number of O and Mg to be -2 and +2 as in an elementary chemistry textbook, three holes associated with a neutral Cr vacancy should change the oxidation number of three Cr from +3 to +4. Since the ionic radius of the Cr^{4+} ion (69 pm) is smaller than that of Cr^{3+} ion (76 pm),²³ the atomic relaxation to decrease the O-Cr bond

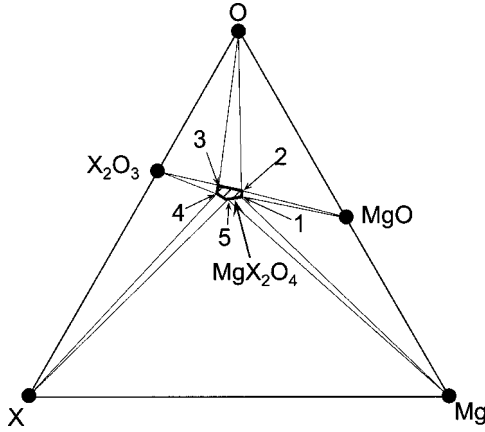


FIG. 1. Schematic ternary phase diagram of the Mg-X-O system ($X = \text{Cr/Al}$).

length is expected to take place. On the other hand, holes associated with the neutral Al vacancy cannot change the oxidation state of Al, since Al^{3+} is the only available state. Of course the reality is more complicated, but not too much. Cluster calculations using atomic orbitals as basis functions in our previous study⁵ found that the major part of the wave function in which holes are expected to be present is located around the oxygen ions surrounding the Al vacancy in the case of MgAl_2O_4 . On the other hand in MgCr_2O_4 , the wave function is located both around Cr and O ions. The electronic mechanism behind the reduction of the Cr-O bond length can therefore be explained by the decrease in the charge density around the Cr ions which reduces the magnitude of shielding of the nuclear charge to contract the ionic size.

C. Formation energy of Cr/Al vacancy in $\text{MgCr}_2\text{O}_4/\text{MgAl}_2\text{O}_4$

Experimental results for MgCr_2O_4 suggest preferred evaporation of Cr to introduce Cr vacancies when annealed in air. On the other hand, MgAl_2O_4 is known not to form Al vacancies alone. Only Schottky type vacancy pairs are thought to be formed under the thermal equilibrium condition. The electronic mechanism behind the stabilization of the Cr vacancies in MgCr_2O_4 is of great interest.

The formation energy of a neutral vacancy in a compound in general depends on the atomic chemical potentials of the system. The formation energy of a metal vacancy can be given by^{24,25}

$$E_V^F = E_t[\text{Mg}_n\text{X}_{2n-1}\text{O}_{4n}] - E_t[\text{Mg}_n\text{X}_{2n}\text{O}_{4n}] + \mu_X, \quad (2)$$

where E_t is the total energy of the supercell with/without a defect. μ_X is the chemical potential of the X atom ($X = \text{Al}$ or Cr). $n = 8$ in the present work. μ_X varies depending upon the chemical environment of the system. Figure 1 schematically shows the phase diagram of the ternary system Mg-X-O. Chemical potentials of three elements should be correlated each other to satisfy the following equation:

$$\mu_{\text{Mg}} + 2\mu_X + 4\mu_{\text{O}} = \mu_{\text{MgX}_2\text{O}_4(\text{bulk})}. \quad (3)$$

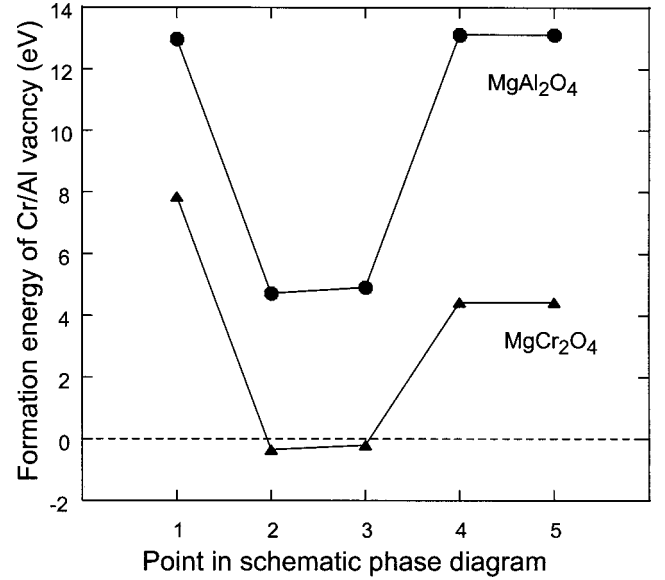


FIG. 2. Theoretical formation energy of X-site vacancies in MgX_2O_4 ($X = \text{Cr/Al}$) calculated for points indicated in Fig. 1.

Five points indicated in the diagram correspond to the vertices of the three-phase regions. μ_X at these five points can be given as follows:

$$\text{Point 1: } \mu_X = [\mu_{\text{MgX}_2\text{O}_4(\text{bulk})} - 4\mu_{\text{MgO}(\text{bulk})} + 3\mu_{\text{Mg}(\text{bulk})}]/2, \quad (4)$$

$$\text{Point 2: } \mu_X = [\mu_{\text{MgX}_2\text{O}_4(\text{bulk})} - \mu_{\text{MgO}(\text{bulk})} - 3\mu_{\text{O}(\text{bulk})}]/2, \quad (5)$$

$$\text{Point 3: } \mu_X = [\mu_{\text{X}_2\text{O}_3(\text{bulk})} - 3\mu_{\text{O}(\text{bulk})}]/2, \quad (6)$$

$$\text{Point 4,5: } \mu_X = \mu_{X(\text{bulk})}. \quad (7)$$

Chemical potentials for the bulk substances in these equations were obtained as the total energies per unit formula by separate calculations in the present study.

Some other phases have been reported in the ternary phase diagrams, such as Al_3Mg_2 and $\text{Al}_{12}\text{Mg}_{17}$ in the Mg-Al binary, and CrO_2 and CrO in the Cr-O binary. We did not consider the equilibrium with these compounds assuming that the heat of formation of these compounds does not change the formation energies of present interest significantly.

Theoretical formation energy of the X vacancy is plotted in Fig. 2 at five points as indicated in Fig. 1. As a general trend in metal oxides, the formation energy of a metal vacancy is smaller in the oxygen-rich conditions, such as at points 2 and 3. The difference in the formation energies between points 1 and 2 corresponds to 1.5 times the heat of formation of MgO , $\Delta H(\text{MgO})$, as defined by

$$\Delta H(\text{MgO}) = \mu_{\text{MgO}(\text{bulk})} - (\mu_{\text{Mg}(\text{bulk})} + \mu_{\text{O}(\text{bulk})}). \quad (8)$$

The meaning of Eq. (8) is identical to that of Eq. (1), since we use total energy E_t as the chemical potential, μ in Eq. (8). Theoretical $\Delta H(\text{MgO})$ in the present work is -5.49 eV/unit formula, which corresponds to experimental enthalpy of for-

mation of MgO at 298 K, i.e., -6.24 eV/unit formula.²² The difference in the formation energies between points 3 and 4 corresponds to 0.5 times of the heat of formation of X_2O_3 , $\Delta H(X_2O_3)$. The theoretical $\Delta H(Al_2O_3)$ is -16.42 eV/unit formula, which corresponds to experimental enthalpy of formation at 298 K, i.e., -17.37 eV/unit formula.²² The theoretical $\Delta H(Cr_2O_3)$ is -9.18 eV and -11.81 eV/unit formula by experiment at 298 K.²²

The difference between the formation energy of a Cr/Al vacancy is smaller in $MgCr_2O_4$ by 5.11 eV at points 1 and 2, 5.09 eV at point 3, and 8.71 eV at points 4 and 5. As a result, the formation energies became negative values at points 2 and 3 in $MgCr_2O_4$. This is in good contrast to the large formation energies even in the oxygen-rich limits in $MgAl_2O_4$, i.e., 4.76–4.92 eV.

The theoretical formation energies well explain the experimental results of $MgCr_{2-x}O_4$ showing wide nonstoichiometry in the range of $0 < x < 0.49$ at 2573 K in air. Another set of experiments to synthesize nonstoichiometric $MgCr_{2-x}O_4$ in the range of $0 < x < 0.20$ has been successful in air,⁴ which also confirms the abundance of Cr vacancies in an oxidizing environment.

IV. SUMMARY

We made first-principles pseudopotential calculations using plane-wave basis functions in order to quantitatively evaluate the formation energy of Cr/Al vacancies in $MgCr_2O_4$ and $MgAl_2O_4$ within GGA. Relaxation of atoms within the second nearest neighbor shell of the vacancy was taken into account in a 56-atom supercell. The formation energy was calculated as a function of the atomic chemical potential of Cr/Al. It shows negative values in the case of the oxidation limit of $MgCr_2O_4$. On the other hand, the formation energy of the Al vacancy in $MgAl_2O_4$ under the same condition is as large as 4.76 eV. These results provide quantitative rationale of the difference in the formation energy of X site vacancy in two compounds: Cr vacancies are abundant in $MgCr_2O_4$ when annealed in air, while Al vacancies alone are not present in $MgAl_2O_4$.

ACKNOWLEDGMENTS

This work is supported by a Grant-in-Aid for Scientific Research on Priority Areas (Grant No. 751) from the Ministry of Education, Science, Sports and Culture of Japan.

-
- ¹A. M. Alper, R. N. McNally, R. C. Doman, and F. G. Keihn, *J. Am. Ceram. Soc.* **47**, 30 (1964).
²H. Moriwake, T. Hata, M. Katsumata, M. Takahashi, and I. Shimono, *J. Ceram. Soc. Jpn.* **107**, 541 (1999).
³H. Moriwake, T. Hata, M. Takahashi, and I. Shimono, *J. Ceram. Soc. Jpn.* **107**, 850 (1999).
⁴H. Moriwake, T. Hata, M. Katsumata, M. Takahashi, and I. Shimono, *J. Ceram. Soc. Jpn.* **107**, 258 (1999).
⁵H. Moriwake, I. Tanaka, F. Oba, and H. Adachi, *Jpn. J. Appl. Phys.* **39**, 513 (2000).
⁶R. S. Mulliken, *J. Chem. Phys.* **23**, 1833 (1955).
⁷H. Sawada, *Mater. Res. Bull.* **31**, 361 (1996).
⁸H. Sawada, *Mater. Res. Bull.* **30**, 341 (1995).
⁹T. R. McGuire, L. N. Howard, and J. S. Smart, *Ceram. Age* **60**, 22 (1952).
¹⁰E. Whipple and A. Wood, *J. Inorg. Nucl. Chem.* **24**, 23 (1962).
¹¹G. Blasse and J. F. Fast, *Philips Res. Rep.* **18**, 393 (1962).
¹²H. Shaked, J. M. Hasting, and L. M. Corliss, *Phys. Rev. B* **1**, 3116 (1962).
¹³S. Ligenza and H. Ptasiwicz-Bak, *Phys. Status Solidi* **90**, 310 (1978).
¹⁴P. Blaha, K. Schwarz, and J. Luitz, WIEN97, A Full Potential Linearized Augmented Plane Wave Package for Calculating Crystal Properties (Karlheinz Schwarz, Technical University Wien, Vienna, 1999).
¹⁵J. P. Perdew, J. A. Chevary, S. H. Vosko, K. A. Jackson, M. R. Pederson, D. J. Singh, and C. Fiolhais, *Phys. Rev. B* **46**, 6671 (1992).
¹⁶V. Milman, B. Winkler, J. A. White, C. J. Pickard, M. C. Payne, E. V. Akhmatkaya, and R. H. Nobes, *Int. J. Quantum Chem.* **77**, 895 (2000). The present calculations were performed using the CASTEP program code (Molecular Simulations, Inc., San Diego, CA).
¹⁷D. Vanderbilt, *Phys. Rev. B* **41**, 7892 (1990).
¹⁸G. Kresse and J. Furthmüller, *Phys. Rev. B* **54**, 11169 (1996).
¹⁹M. C. Payne, M. P. Teter, D. C. Allan, T. A. Arias, and J. D. Joannopoulos, *Rev. Mod. Phys.* **64**, 1045 (1992).
²⁰W. H. Press, S. A. Teukolsky, W. T. Vetterling, and B. P. Flannery, *Numerical Recipes*, 2nd ed. (Cambridge University Press, Cambridge, 1992), p. 418.
²¹C. S. Barrett, L. Meyer, and J. Wasserman, *J. Chem. Phys.* **47**, 592 (1967).
²²*NIST Chemistry WebBook, NIST Standard Reference Database Number 69*, edited by W. G. Mallard and P. J. Linstrom (National Institute of Standards and Technology, Gaithersburg, MD, 2000).
²³R. D. Shannon, *Acta Crystallogr., Sect. A: Cryst. Phys., Diffraction, Theor. Gen. Crystallogr.* **32**, 751 (1976).
²⁴S. B. Zhang, S.-H. Wei, A. Zunger, and H. Katayama-Yoshida, *Phys. Rev. Lett.* **67**, 2339 (1991).
²⁵D. B. Lanks, C. G. Van de Walle, G. F. Neumark, P. E. Blochl, and S. T. Pantelides, *Phys. Rev. B* **45**, 10 965 (1992).